ELSEVIER

Journal of Contaminant Hydrology 16 (1994) 319–337

JOURNAL OF
Contaminant
Hydrology

Cation transport in natural porous media on laboratory scale: multicomponent effects

Miroslav Černík, Kurt Barmettler, Daniel Grolimund, Werner Rohr, Michal Borkovec*, Hans Sticher

Institute of Terrestrial Ecology, Federal Institute of Technology (ETH), Grabenstrasse 3, CH-8952 Schlieren, Switzerland

(Received December 6, 1993; revision accepted April 27, 1994)

Abstract

Multicomponent transport experiments were performed with four major cations, Na^+, K^+, Ca^{2+} and Mg^{2+}, in laboratory columns packed with a non-calcareous soil. The breakthrough curves are explained quantitatively with a box model including cation exchange. We use a single set of selectivity coefficients, an independently verified value of the cation-exchange capacity (CEC), and an adjusted value of the Péclet number. This Péclet number is smaller than the value determined from independent tracer experiments. The model is able to predict all experimentally observed breakthrough curves quite well. The selectivity coefficients determined from binary exchange experiments prove unreliable for the prediction of multicomponent experiments. We propose to estimate the selectivity coefficients by directly fitting the multicomponent breakthrough curves. Their shape is a very sensitive function of the values of these coefficients. Concepts from non-linear chromatography can be used in order to interpret several qualitative features of the breakthrough curves.

1. Introduction

Modeling reactive transport in porous media has become an increasingly important tool for quantitative predictions of pollutant fate in soils, aquifers and fractured rocks. In recent years much progress was made in the description of transport of conservative tracers on the laboratory and field scale. Such solutes which adsorb very weakly on the solid matrix (e.g., chloride, nitrate) are transported by pore-water flow. Over a limited spatial and temporal scale the transport of such conservative tracers can be often modeled with the convection–dispersion equation (Dagan, 1989). Most

* Corresponding author.

SSDI 0169-7722(94)0000-0

environmentally relevant chemicals, however, adsorb more or less strongly on the solid matrix with the consequence that the migration of such non-conservative tracers is slowed down. In the simplest case of linear adsorption, no competition and no chemical reactions in solution, the different chemicals move independently as conservative tracers but with velocities which are reduced with respect to the velocity of a conservative tracer by the so-called retardation coefficient (Sardin et al., 1991). For inorganic sorbents, however, this case is rather an exception since adsorption isotherms are non-linear and different solutes compete for the same sorption sites. Such effects lead to wealth of non-linear chromatographic phenomena such as formation of self-sharpening or self-broadening fronts and simultaneous concentration changes of several components in the retarded fronts (Helfferich and Klein, 1970; Schweich et al., 1993). While in the context of pollutant transport the development of numerical codes for the solution of transport coupled to chemical equilibria has reached a high degree of sophistication (Jauzein et al., 1989; Yeh and Tripathi, 1989; Gaston and Selim, 1990; Schulin et al., 1991; Bjerg et al., 1993; Mansell et al., 1993) the elementary understanding of the observed breakthrough patterns in terms of basic concepts of non-linear chromatography has advanced much more reluctantly (Charbenau, 1981; Schweich and Sardin, 1981; Valocchi et al., 1981; Appelo et al., 1993; Schweich et al., 1993).

Probably the simplest example of such non-linear, multicomponent phenomena in natural porous media is transport processes of major cations. As such cations (e.g., Na^+, Ca^{2+}, Mg^{2+}) occur in relatively high concentrations, one obtains rather small retardation coefficients which can be determined either in the laboratory or in the field. Sorption processes can be modeled as exchange reactions (each characterized by a selectivity coefficient) involving a single site of a concentration which is related to the cation-exchange capacity (CEC) (Rainwater et al., 1987; Jardine et al., 1988; Bond and Phillips, 1990; Schulin et al., 1991). Sardin et al. (1986) and Jauzein et al. (1989) have shown that apparently complicated laboratory column breakthrough curves can be explained by solving the coupled transport and exchange equations of the species involved. They have also interpreted the breakthrough curves by applying concepts originating from non-linear chromatography. On the field scale, Valocchi et al. (1981) and Bjerg et al. (1993) were able to predict transport behaviour of major cations by applying very similar techniques.

In the present study we investigate multicomponent cation transport of four major cations, Na^+, K^+, Ca^{2+} and Mg^{2+}, in laboratory columns with a non-calcareous soil as solid matrix. Here, we attempt to explain several different experimental breakthrough curves with a single set of parameters and confirm that column experiments can be used to measure exchange capacities and selectivity coefficients as proposed recently (Schweich et al., 1983; Griffioen et al., 1992; Bürgisser et al., 1993). Furthermore, we demonstrate that concepts from non-linear chromatography can be used in order to interpret the measured breakthrough curves.

2. Theory

Consider a chromatographic column filled with a soil material and saturated with

water. Suppose that the system contains M different species i. These species have concentrations in the solution c_i (in moles per litre) and their amount adsorbed on the solid phase is q_i (in moles per gram). The evolution of the concentration profiles (being a function of time t and depth x) can be described by a set of convection–dispersion equations:

$$\frac{\partial c_i}{\partial t} + \rho \frac{\partial q_i}{\partial t} = D \frac{\partial^2 c_i}{\partial x^2} - v \frac{\partial c_i}{\partial x}, \qquad \text{for} \qquad i = 1, \ldots, M \tag{1}$$

where D is the dispersion coefficient of the medium; v the microscopic pore-water velocity; and ρ the mass of sorbent per unit pore volume. For a conservative tracer ($q_i = 0$) the response of the column upon a step change in concentration at column input ($x = 0$) results in a sigmoidal concentration increase at the column outlet ($x = L$). The breakthrough is centered at a time L/v, which leads to the natural dimensionless time tv/L of the problem. This quantity is also equivalent to V/V_0 which is the ratio of the cumulative volume of solvent eluted V and the pore volume V_0. The square of the relative width of the breakthrough curve of a conservative tracer (coefficient of variance) is given by the inverse of the column Péclet number $\mathrm{Pe} = vL/D$. With increasing Péclet number, the magnitude of dispersion effects will decrease and the breakthrough approaches a step function (Villermaux, 1981).

In the present study we employ a box model (mixing cell model) in order to obtain approximate solutions of the convection–dispersion equations coupled to chemical equilibria. In this model, the chromatographic column is represented by well-stirred reactors in series. The mass-balance equation for the mixing cell $j = 1, \ldots, J$ reads (Sardin et al., 1991):

$$\frac{\mathrm{d}c_i^{(j)}}{\mathrm{d}t} + \rho \frac{\mathrm{d}q_i^{(j)}}{\mathrm{d}t} = \frac{vJ}{L}\left(c_i^{(j-1)} - c_i^{(j)}\right) \tag{2}$$

where the superscript indicates the cell number ($c_i^{(0)}$ represents the concentration in the feed). For sufficiently high Péclet number (approx. $\mathrm{Pe} \geqslant 50$) the solutions of the convection–dispersion equation (1) are very well approximated by the solutions of the box-model equation (2) by setting (Villermaux, 1981; Sardin et al., 1991; Bajracharya and Barry, 1993):

$$\mathrm{Pe} = 2J \tag{3}$$

Note that the box-model equation (2) is essentially equivalent to a first-order difference approximation of the convective part of Eq. 1. In a sense, dispersion arises from the discretization of the convective part.

In order to include sorption effects in the present study, let us assume chemical equilibrium between dissolved and adsorbed components. Thus, q_i depends solely on the solution composition, and therefore:

$$\frac{\partial q_i}{\partial t} = \sum_{k=1}^{M} \frac{\partial q_i}{\partial c_k} \frac{\partial c_k}{\partial t} \tag{4}$$

In the case of independent solutes obeying a linear adsorption isotherms (i.e. $q_i = K_i c_i$, where K_i is the partition coefficient of component i) we find from Eq. 4

that Eq. 1 decouples. Each sorbing chemical moves independently and behaves like a conservative tracer which is slowed down by the retardation coefficient:

$$R_i = 1 + \rho K_i \tag{5}$$

In the case of interacting solutes and non-linear adsorption isotherms, the individual retardation coefficients are no longer constant and the solution of the set of coupled differential equations (2) and (4) must be obtained numerically. Nevertheless, the multicomponent breakthrough bears some characteristic features (Helfferich and Klein, 1970; Schweich et al., 1993). After a step change input, the elution curve is generally composed of several regions where the composition of the outflow solution remains constant. These constant concentration zones are separated by regions, called fronts, where the composition of the outflow solution changes. The concentration changes between these fronts are usually either gradual or sudden. In the case of a gradual change one commonly deals with a self-broadening front (or a diffuse front). In the case of a sudden change, one is either confronted with a self-sharpening front or an indifferent front. The distinction between these sudden fronts is related to their dispersion characteristics (Schweich et al., 1993). As a rule of thumb, retarded sudden concentration changes usually correspond to a self-sharpening front while non-retarded sudden changes are indifferent fronts. Non-retarded fronts are related mostly to changes of a conserved quantity which involves only dissolved species which do not participate in the sorption reactions (e.g., conservative tracer, total solution normality). Retarded fronts, on the other hand, are related to conserved quantities which involve solution species as well as species which participate in sorption processes. Conserved quantities, which involve adsorbed species only, do generally not lead to an experimentally observable front. In a given experimental breakthrough curve one may not be able to distinguish all these fronts (Schweich et al., 1993).

In the present article we shall focus on ion-exchange reactions of four major cations, Na^+, K^+, Ca^{2+} and Mg^{2+}. In the case of a single ion-exchange site X we have to consider the following six exchange reactions, namely:

$$K^+ + NaX \rightleftharpoons Na^+ + KX, \qquad K_{K/Na}$$

$$Ca^{2+} + 2NaX \rightleftharpoons 2Na^+ + CaX_2, \qquad K_{Ca/Na}$$

$$Mg^{2+} + 2NaX \rightleftharpoons 2Na^+ + MgX_2, \qquad K_{Mg/Na}$$

$$Mg^{2+} + CaX_2 \rightleftharpoons Ca^{2+} + MgX_2, \qquad K_{Mg/Ca}$$

$$Ca^{2+} + 2KX \rightleftharpoons 2K^+ + CaX_2, \qquad K_{Ca/K}$$

$$Mg^{2+} + 2KX \rightleftharpoons 2K^+ + MgX_2, \qquad K_{Mg/K}$$

where we have added the corresponding selectivity coefficients (defined below) for later reference. The first reaction involves the exchange of cations of the same valency

and the obvious choice of the exchange constant is:

$$K_{K/Na} = \frac{c_{Na} q_K}{q_{Na} c_K} \tag{6}$$

For the second and third reaction, where cations of different valencies are exchanged, several equilibrium relations have been proposed (Bolt, 1967) and we employ the natural extension of the above relation, namely:

$$K_{Ca/Na} = 2Q \frac{c_{Na}^2 q_{Ca}}{q_{Na}^2 c_{Ca}} \tag{7}$$

$$K_{Mg/Na} = 2Q \frac{c_{Na}^2 q_{Mg}}{q_{Na}^2 c_{Mg}} \tag{8}$$

where Q denotes the cation-exchange capacity (CEC) in mole charge per solid mass. By introducing the factor $2Q$ all selectivity coefficients are now defined according to the Gaines–Thomas convention which is frequently used in the context of cation transport (Valocchi et al., 1981; Sardin et al., 1986; Appelo et al., 1990; Bjerg et al., 1993).

The selectivity coefficients of the last three reactions are not independent from the previous reactions and can be expressed in terms of their selectivity coefficients $K_{K/Na}$, $K_{Ca/Na}$ and $K_{Mg/Na}$ as:

$$K_{Mg/Ca} = \frac{c_{Ca} q_{Mg}}{q_{Ca} c_{Mg}} = \frac{K_{Mg/Na}}{K_{Ca/Na}} \tag{9}$$

$$K_{Ca/K} = 2Q \frac{c_K^2 q_{Ca}}{q_K^2 c_{Ca}} = \frac{K_{Ca/Na}}{K_{K/Na}^2} \tag{10}$$

$$K_{Mg/K} = 2Q \frac{c_K^2 q_{Mg}}{q_K^2 c_{Mg}} = \frac{K_{Mg/Na}}{K_{K/Na}^2} \tag{11}$$

In this system involving four cations and one surface site, five mass-balance equations must be satisfied. The chemical equilibrium described by the set of three mass-action and five mass-balance equations can be employed in the solution of the box-model equation (2). A numerical scheme for the solution was implemented by Jauzein et al. (1989) in the IMPACT code which was also used in this study. In this special case, one of the five mass-balance equations (which is related to the CEC) involves adsorbed species only and therefore we expect up to four fronts in total. Another of these five mass-balance equations is proportional to the total normality and thus involves solution species only. Therefore, one front will be non-retarded (normality front) while the other three will be retarded.

Binary exchange column experiments at constant normality represents a useful tool for the determination of exchange capacity and of the selectivity coefficient of a given cation pair. As we employ this technique here, let us review the relevant concepts. Details can be found in Schweich et al. (1983), Griffioen et al. (1992) and Bürgisser et

al. (1993). In a step experiment where, at constant normality, the dissolved cation is changed (e.g., from Na^+ to K^+), one can obtain the CEC from the retardation of the breakthrough curve. The retardation coefficient R is experimentally accessible by integrating the experimental breakthrough curve and is related to the CEC by (Schweich et al., 1983):

$$Q = c_0(R - 1)/\rho \tag{12}$$

where c_0 is the overall normality of the solution (i.e. twice the molarity for a divalent cation). Eq. 12 is the application of the fact that the retardation coefficient is given by the ratio between the total amount of a given component (adsorbed and dissolved) and the amount in solution.

The selectivity coefficient can be extracted from the self-broadening part of the breakthrough curve. Each experimental point in this front represents a measurement of retardation coefficient $R(c)$ as a function of the solution concentration c. Integration of this retardation coefficient yields directly the exchange isotherm:

$$q(c) = \rho^{-1} \int_0^c [R(c') - 1] \mathrm{d}c' \tag{13}$$

The resulting exchange isotherm can be fitted with corresponding expressions. From Eq. 6 one obtains the isotherm for the exchange of Na^+ by K^+, which reads:

$$q_K = Q \frac{K_{K/Na} c_K}{c_0 + c_K(K_{K/Na} - 1)} \tag{14}$$

where c_0 is the constant normality of the solution. For the exchange of Na^+ by Ca^{2+} (or Mg^{2+}) the isotherm:

$$q_{Ca} = \frac{Q}{2} \left[1 + \frac{(c_0 - 2c_{Ca})^2}{2K_{Ca/Na} c_{Ca}} - \left\{ \left(1 + \frac{(c_0 - 2c_{Ca})^2}{2K_{Ca/Na} c_{Ca}} \right)^2 - 1 \right\}^{1/2} \right] \tag{15}$$

follows from Eq. 7. As discussed by Griffioen et al. (1992) and Bürgisser et al. (1993), the present method for the determination of the isotherms neglects dispersion effects and can be applied only to columns of a sufficiently high Péclet number (typically $Pe > 50$).

3. Experiments

3.1. Soil material

For the column experiments we have used a soil material originating from a weakly developed non-calcareous argillic horizon (depth of 36–46 cm) of an orthic Luvisol (Arenic Hapludalf). Below this horizon one finds a well-developed argillic horizon and the C horizon with 70% of gravel. The site is located in northern Switzerland close to the river Rhine (Ellikon-am-Rhein, Winzlerboden). The soil material was dried at 40°C and sieved by hand through a 2-mm sieve. The sieved material contains

16% clay, 14% silt and 70% sand, is quite acidic (pH = 4.7 in 0.01 mol L^{-1} $CaCl_2$), carbonate free and has an organic carbon content of 0.3%.

The mineralogy was analysed by powder X-ray diffraction on a Scintag® diffractometer (XRD *2000*) with a Cu-K_α line as radiation source and an energy discriminating detector. Samples from the clay fraction (< 2 μm) were X-rayed either untreated, heated to 550°C or treated with ethylene glycol. Comparison of the spectra shows (Whittig and Allardice, 1986) that it contains mainly kaolinite, vermiculite and quartz with traces of feldspars, illite and goethite.

3.2. Preparation of the columns

Aggregates of 200–630 μm were obtained by subsequent sieving. These aggregates have a specific surface area of 10.7 m^2 g^{-1} (BET) and a matrix density of 2600 kg m^{-3}. The aggregates were mixed with an inert matrix (sieved cristobalite sand, 250–500 μm) at a proportion of 23% of aggregates (w/w). This mixing procedure is required in order to avoid column clogging but does not influence the breakthrough behaviour of the cations investigated. The mixed material was filled into a glass chromatography columns of 1.5–1.7 cm in diameter (Omni®) to a height of 40–50 cm. The columns were purged with CO_2 and saturated by upward flow with $CaCl_2$ solution (0.5 *M*) until all gas bubbles disappeared. The solutions were always pumped by a HPLC pump (S*1000*, Sykam®) through a degasser (ERC-*3511*, Erma®) into the columns. Flow rates of 1.7–2.4 mL min^{-1} were used in all experiments. Microbial activity was inhibited by flushing the column with NaN_3 (0.015 mol L^{-1}) solution between the experiments and keeping the feeding solutions in contact with air.

3.3. Column experiments with conservative tracers

Pore volume and the Péclet number of the column were determined by pulse experiments with conservative tracers. Tracer solutions ($NaNO_3$, NaBr) were injected into a column saturated with $CaCl_2$ (0.5 mol L^{-1}) from a 25-μL sample loop. The breakthrough curves were measured on-line by a UV spectrometer (UVIS *204* Linear®). As the measured breakthrough was essentially identical for both tracers we deduce that tracers behave conservatively. From the first and second moments of the essentially Gaussian breakthrough curves (Villermaux, 1981) travel velocities of $(3–5)\cdot10^{-4}$ m s^{-1} and pore volumes of 30–40 mL were determined. We obtain a kinematic porosity $\theta \approx 0.48$, and a dispersion coefficient D of $(4.3 \pm 0.2)\cdot10^{-7}$ m^2 s^{-1}. From these values we obtain the amount of soil per unit pore volume $\rho \approx 620$ kg m^{-3} and the column Péclet number Pe = 409. For subsequent calculations Pe ≈ 400 was used.

3.4. Column experiments with cations

Experiments were performed as a sequence of two step changes of solutions feeding the column. Columns flushed with $CaCl_2$ (0.5 mol L^{-1}) for a few days were equilibrated with solution *1* (until the input and output concentrations of all components were identical) and

Table 1
Summary of column experiments performed

Experiment	Solution *1*				Solution *2*			
	Na^+	K^+	Ca^{2+}	Mg^{2+}	Na^+	K^+	Ca^{2+}	Mg^{2+}
1	25	–	–	–	–	25	–	–
2	25	–	–	–	–	–	12.5	–
3	25	–	–	–	–	–	–	12.5
4	26	–	–	–	–	–	5.4	–
5	–	–	12.5	–	–	–	–	12.5
6	–	–	–	12.5	–	25	–	–
7	–	–	12.5	–	–	25	–	–
8	1.2	–	4.9	2.1	–	14.3	–	4.6
9	–	–	–	14	1.9	3.0	2.2	–

The column equilibrated with solution *1* was fed with solution *2*. After equilibration the feed was changed back to solution *1*. All concentrations are in mmol L^{-1}.

then the feed was changed to solution *2*. This time defines the start of the experiment. After the equilibration of the column with solution *2*, the feed solution was changed back to solution *1*. The column outflow was collected in portions of 6 mL with a fraction collector (Pharmacia®) and analyzed for Na^+, K^+, Ca^{2+} and Mg^{2+} by a sequential inductively coupled plasma–atomic emission spectrometry (ICP–AES) (Liberty *200*, Varian®). This sample size is small enough to be neglected with respect to the dispersion of the column.

All nine experiments performed are summarized in Table 1, where compositions of the feed solutions *1* and *2* are given. The solutions were prepared from the chloride salts of the corresponding cations (Merck®, p.a.) by dissolution in water obtained from a Nanopure® apparatus. Exps. *1–7* are binary exchange experiments. Exp. *4* involves a change in total normality while exps. *1–3* and exps. *5–7* are carried out at constant total normality of 25 mmol L^{-1}. Exps. *8* and *9* represent more complicated multicomponent experiments. The experimental results were well reproducible as checked with additional experiments with newly packed columns.

The CEC determined from column experiments was verified independently by applying a standard procedure with ammonium acetate (Page et al., 1982).

4. Results and discussion

4.1. Binary exchange experiments

In the first part of the study, binary exchange column experiments were performed (exps. *1–7*, see Table 1). The breakthrough curve of the monovalent–monovalent exchange of Na^+ displaced with K^+ (exp. *1*) is shown in Fig. 1a. The column equilibrated with 25 mmol L^{-1} Na^+ solution was fed with K^+ solution of the same normality. As the column was saturated with Na^+, the outflow solution contains only Na^+ at first. Approximately after 2.5 pore volumes the composition of the outflow

solution changes suddenly to pure K^+ which corresponds to the composition of the feeding solution. Since K^+ in the feed is exchanged by Na^+ from the exchanger, this front appears retarded. The retardation coefficient is proportional to the ratio of CEC to normality of solution (cf. Eq. 12).

After 5 pore volumes the solution was changed back to Na^+ solution (arrow in Fig. 1a). Now already after one pore volume the K^+ concentration starts to decrease and the concentrations approach gradually the final composition of the feed. The appearance of the exchange fronts shown in Fig. 1a demonstrates the difference between a self-sharpening front (sudden change from the Na^+ solution to the K^+ solution) and self-broadening front (very gradual change from the K^+ solution to the Na^+ solution). A self-sharpening front will appear if the affinity of the exchanger for the injected cation (K^+) is higher than the affinity for the cation which is adsorbed on the exchanger (Na^+). In the reverse situation, a self-broadening front will form. This means that the ion-exchange isotherm for K^+ is convex and the exchange coefficient $K_{K/Na}$ is larger than 1.

From the experimental breakthrough curve shown in Fig. 1a the CEC and the selectivity coefficient $K_{K/Na}$ were obtained according to the following procedure. The retardation coefficient can be read directly from the position of the sharp front and amounts to $R \approx 2.5$. The results of the more accurate numerical integration of the experimental curve are given in Table 2. While the retardation coefficients for the first and second part of the experiment should be identical, the retardation coefficient

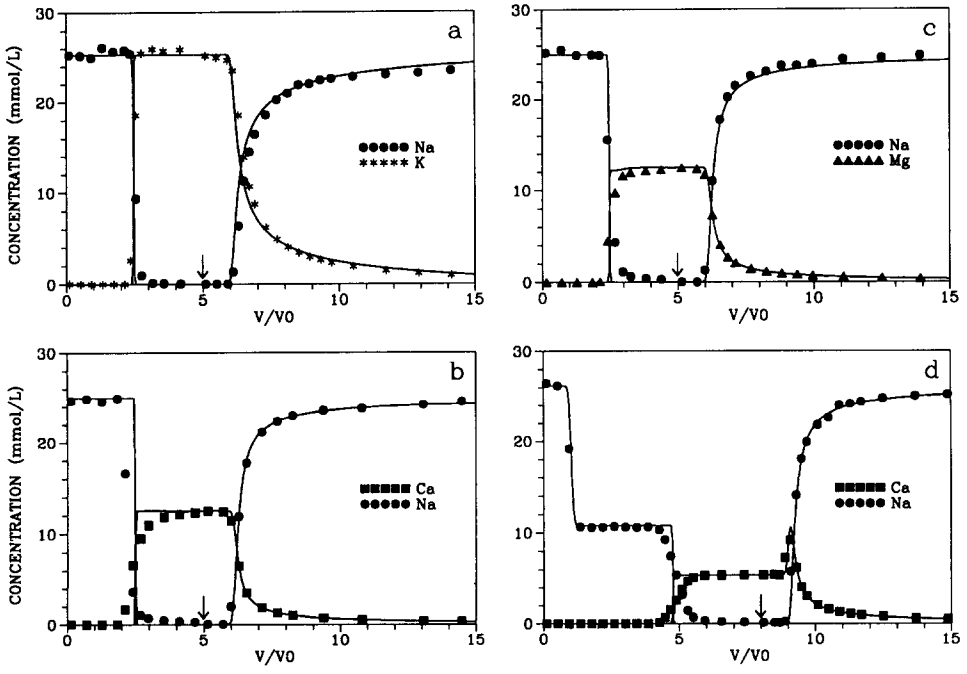

Fig. 1. Experimetal data (*symbols*) and model calculations (*solid lines*) for binary exchange breakthrough curves with set *1* and Pe = 400: (a) exp. *1*; (b) exp. *2*; (c) exp. *3*; and (d) exp. *4*.

Table 2
Retardation coefficients obtained by integration of the breakthrough curves of binary exchange experiments

Experiment	Cation pair	R_1	R_2
1	Na^+–K^+	2.49	2.39
2	Na^+–Ca^{2+}	2.48	2.09
3	Na^+–Mg^{2+}	2.52	2.23
5	Mg^{2+}–Ca^{2+}	2.41	2.53
6	Mg^{2+}–K^+	2.43	2.47
7	Ca^{2+}–K^+	2.48	2.23
	Mean value	$\overline{2.47 \pm 0.04}$	–

By changing the feed from the first to the second solution and back, we have obtained retardation coefficients R_1 and R_2, respectively. The mean value of the retardation coefficients for the self-sharpening parts of the breakthrough curves gives a CEC of 59 mmol kg^{-1}.

estimated from the self-broadening front is usually smaller since the slow decay of the self-broadening front of the breakthrough is more difficult to integrate. Using Eq. 12, we obtain an exchange capacity of 59 ± 1 mmol kg^{-1}. This value of CEC will be used throughout this paper. We shall explain later how this value was verified by independent column experiments. This value is also in good agreement with an independent measurement of 60 ± 1 mmol kg^{-1} obtained from batch samples.

The self-broadening front has been integrated by applying Eq. 13 and the selectivity coefficient determined by fitting the resulting isotherm to Eq. 14. We obtain a value for the selectivity coefficient $K_{K/Na} = 14 \pm 2$ which is given in the first row of Table 3. We now have used this selectivity coefficient $K_{K/Na}$ and the CEC-value of 59 mmol kg^{-1} in order to predict the measured breakthrough curve. The only additional parameter is the Péclet number Pe = 400 as obtained from an independent tracer experiment. We observe a good agreement between the experimental data points and the calculated breakthrough curve (see Fig. 1a). The good agreement is not surprising as the relevant parameters (CEC and $K_{K/Na}$) were determined from the same experimental record.

Similar monovalent–divalent exchange experiments have been performed where Na^+ has been displaced with Ca^{2+} or Mg^{2+} (exps. *2* and *3*). The experimental records are shown in Fig. 1b and c. The normality is kept constant at 25 mmol L^{-1}, which means that the concentration of the divalent cations is 12.5 mmol L^{-1}. Again from the appearance of the breakthrough curve we recognize that the affinity of the exchanger for Ca^{2+} (or Mg^{2+}) is larger than for Na^+. The mean retardation coefficients are given in Table 2. As this quantity is given by the CEC (cf. Eq. 12) its value should be independent of the type of cation. Table 2 confirms that this is true within experimental error. We have applied Eq. 13 for the integration of the self-broadening parts of the breakthrough curve and fitted Eq. 15 in order to obtain the values of the selectivity coefficients $K_{Ca/Na}$ and $K_{Mg/Na}$. The resulting values are given in the first row of Table 3. The CEC and these selectivity coefficients can be used to calculate the breakthrough curves (with Pe = 400) and the results are compared with the

Table 3
Gaines–Thomas selectivity coefficients determined in this study from binary exchange experiments (set *1*) and from multicomponent experiments (set *2*)

	$K_{K/Na}$	$K_{Ca/Na}$ (mol L^{-1})	$K_{Mg/Na}$ (mol L^{-1})	$K_{Mg/Ca}$	$K_{Ca/K}$ (mol L^{-1})	$K_{Mg/K}$ (mol L^{-1})
Set *1*	14	6.4	3.4	0.53	0.032	0.017
Set *2*	10	6.4	5.7	0.89	0.064	0.057
Bjerg et al. (1993)[a,b]		5.0		1.0–1.4	0.03	
Bond and Phillips (1990)[a,c]		12				
Gaston and Selim (1990)[c]		6.1	5.7	0.8		
Sardin et al. (1986)[c]		13				
Schulin et al. (1991)[c]				0.5–0.8		
Schulz and Reardon (1983)[b]		2.7		0.8	0.0014	
Valocchi et al. (1981)[a]		6	3.4			

Literature values for similar materials are included.
Obtained from: [a]batch, [b]field and [c]column experiments.

experimental data in Fig. 1b and c. Again, the agreement is quite good, which is not surprising as the selectivity coefficients have been determined from these experiments. Note that the experimental self-sharpening fronts are broader than the model prediction. We shall return to this point later.

We have now determined the CEC (from three different experiments) and three independent selectivity coefficients. From Eqs. 9–11 we have also obtained the selectivity coefficients for the three other pairs of cations. This set of selectivity coefficients is given in the first row of Table 3 and will be called set *1* for later reference. As the Péclet number is known from an independent tracer experiment (Pe = 400), we should be able to predict the breakthrough of an arbitrarily chosen mixture of these four cations. We now discuss several examples of increasing complexity.

Even though two cations are involved in exps. *1–3* (Fig. 1a–c), we have observed only one retarded front. The other front, which does correspond to the change in normality of the solution, was absent since the experiments were carried out at constant normality. In order to observe both fronts, let us now focus on the situation where the normalities in the feed solutions are different. Such a situation was investigated in exp. *4*, which is shown in Fig. 1d. The column saturated with a Na^+ solution is fed with a Ca^{2+} solution of a lower normality and later changed back to the original Na^+ solution. A similar experiment has been discussed by Jauzein et al. (1989). At first sight, the normality change produces a completely different breakthrough curve which can be predicted very well with the parameters from Table 3. In this case we expect two fronts, namely one non-retarded normality front and one retarded front. As the normality of the displacing Ca^{2+} solution is smaller than the normality of the original Na^+ solution, we observe a decrease in normality after one pore volume (normality front) where the normality of the outflow solution adjusts itself to the normality of the feed, namely to 10.8 mmol L^{-1}. This normality front is followed by the self-sharpening front of the exchange of Na^+ by Ca^{2+} approximately

at 4.5 pore volumes. After the normality front, the exchange of Na^+ by Ca^{2+} is precisely analogous to the results of the experiment at constant normality. However, the retardation coefficient is now larger because the normality of the (final) solution is smaller (cf. Eq. 12). After 8 pore volumes (arrow) the feed is changed back to Na^+ solution of higher normality. Again we expect two fronts. After one pore volume (i.e. at 9 pore volumes total) the normality of the outflow increases to the higher normality of 26 mmol L^{-1} in the feed. The outflow contains 5.4 mmol L^{-1} Ca^{2+}, at first. Later, we observe a Ca^{2+} concentration increase to a constant concentration of 13 mmol L^{-1} Ca^{2+}. The concentration remains constant until the second front sets in. As in the experiment at constant normality, this front is self-broadening and causes the Na^+ concentration to increase and the Ca^{2+} concentration to decrease. The peak in the Ca^{2+} concentration is in fact caused by the appearance of two fronts, namely the normality front (Ca^{2+} concentration increase) and the self-broadening exchange front (Ca^{2+} concentration decrease). If dispersion effects were absent, a very short plateau 0.13 pore volume long would be expected where the Ca^{2+} concentration would remain constant at 13 mmol L^{-1}. The height of the peak is, however, diminished by the presence of dispersion effects. Note that after the normality front, the self-broadening exchange front in exp. *4* (Fig. 1d) is precisely identical to the self-broadening front in exp. *2* (Fig. 1b). Since the selectivity coefficients and CEC have been determined from exp. *2*, it may not seem surprising that exp. *4* (which involves the same exchange process) could be predicted so well without adjustable parameters. Again we remark that the width of the sharp front is predicted to be much narrower than observed in the experiment.

Let us now discuss further experiments and the corresponding predictions without any adjustable parameters (using set *1* which was obtained by fitting the results of exps. *1–3*). In Fig. 2a–c we compare three binary experiments, namely the displacement of Ca^{2+} by Mg^{2+} (exp. *5*, Fig. 2a), of Mg^{2+} by K^+ (exp. *6*, Fig. 2b) and of Ca^{2+} by K^+ (exp. *7*, Fig. 2c). We have also determined the retardation coefficients in these exchange experiments. The values are given in Table 2 and compare well with the previously determined values. This result means that the CEC is indeed the same for any combination of cations. From the rather symmetrical appearance of the data points shown in Fig. 2a–c, one concludes that the selectivity coefficient $K_{Mg/Ca}$ must be rather close to one and the affinities of the exchanger for Ca^{2+}, Mg^{2+} and K^+ must be rather similar. Comparing the predictions, one can see that the model is able to predict the overall position of the breakthrough but the shape of the curves are not predicted very well — particularly, the sharp fronts are always too narrow. We suspect that this effect is kinetic in origin and is due to slow diffusion of the cations into the soil aggregates (Villermaux, 1981; Sardin et al., 1991). Experiments performed at much smaller flow rates have revealed partial sharpening of the fronts but we were facing experimental problems and the results were not very conclusive. Villermaux (1981), Bales and Szecsody (1985), Sardin et al. (1991) and Valocchi (1993) have shown that in the case of a linear isotherm, kinetic effects can be approximated (to first order) as an effective dispersive process with an increased apparent dispersivity. Similar effects can be expected to be operational in the case of non-linear chemical equilibria. Following Wagner et al. (1994) we have therefore decreased the

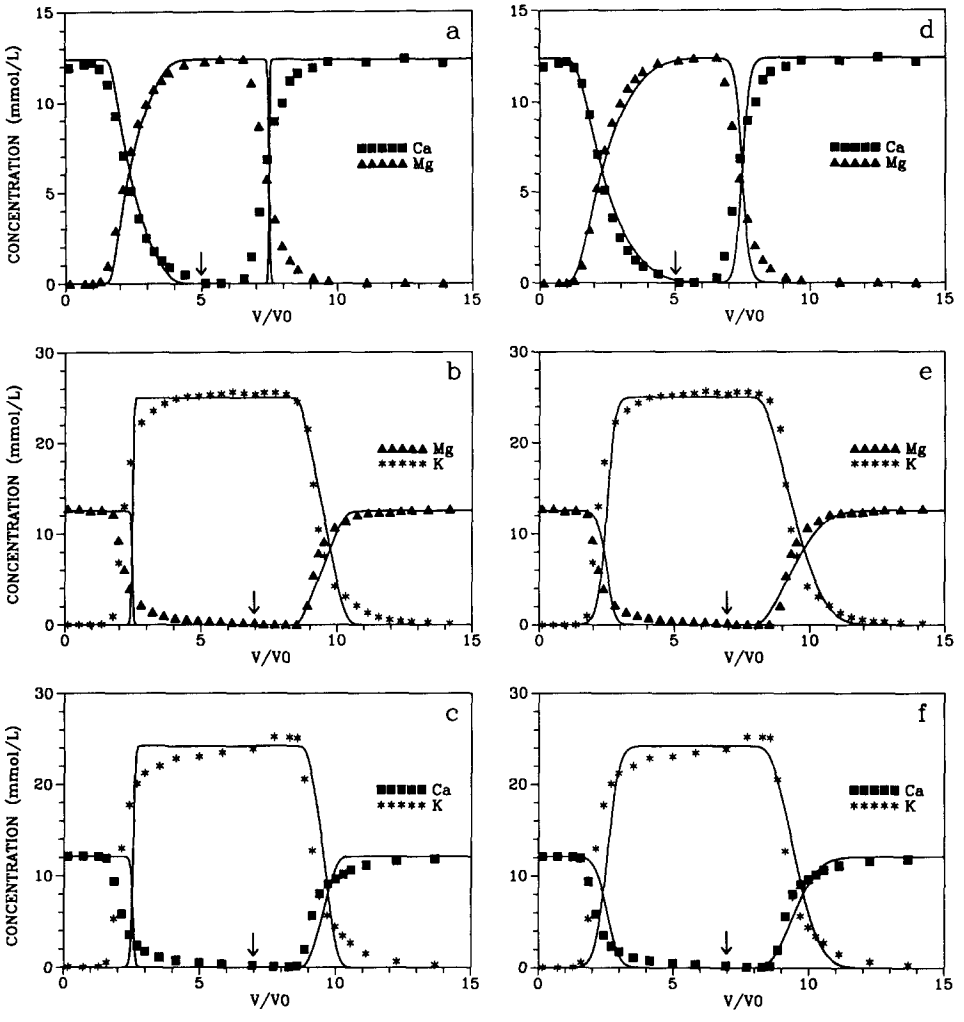

Fig. 2. Experimetal data (*symbols*) and model calculations (*solid lines*) for binary exchange breakthrough curves with set *1* and different Péclet numbers: (a) exp. *5*, Pe = 400; (b) exp. *6*, Pe = 400; (c) exp. *7*, Pe = 400; (d) exp. *5*, Pe = 50; (e) exp. *6*, Pe = 50; and (f) exp. *7*, Pe = 50.

Péclet number from Pe = 400 (Fig. 2a–c, left column) obtained from the tracer experiment to a lower value of Pe = 50 (Fig. 2d–f, right column). One can see that the use of a smaller Péclet number leads to a much better agreement indeed. Still, some details of the breakthrough curves are not well predicted. This disagreement is probably caused by the inaccuracy of such an effective dispersion approximation or by chemical heterogeneity effects. The latter may be particularly important in exps. *6* and *7* (Fig. 2e and f) since sigmoidal exchange isotherm between K^+ and Ca^{2+} or Mg^{2+} (Dufey and Delvaux, 1989) seems to offer the most likely explanation for the shape of the observed breakthrough curves (Schweich and Sardin, 1981). Nevertheless, decreasing the Péclet number to Pe = 50 results into an acceptable description of

the experimental curves. Keeping the fact in mind that no other parameters have been adjusted (i.e. we are using set *1*) the agreement between experiment and model prediction is quite satisfactory. Also exp. *4* which is shown in Fig. 3a can be predicted quite well with this low Péclet number (Pe = 50). This prediction should be compared with calculations with the original value of the Péclet number (Fig. 1d, Pe = 400). Note that the differences are rather minor. Most notably, the widths of the self-sharpening fronts are now somewhat broader. The same applies to all previous exps. *1–3* which can also be well described with Pe = 50. The results of the calculations are not shown but they are not very different from the results shown

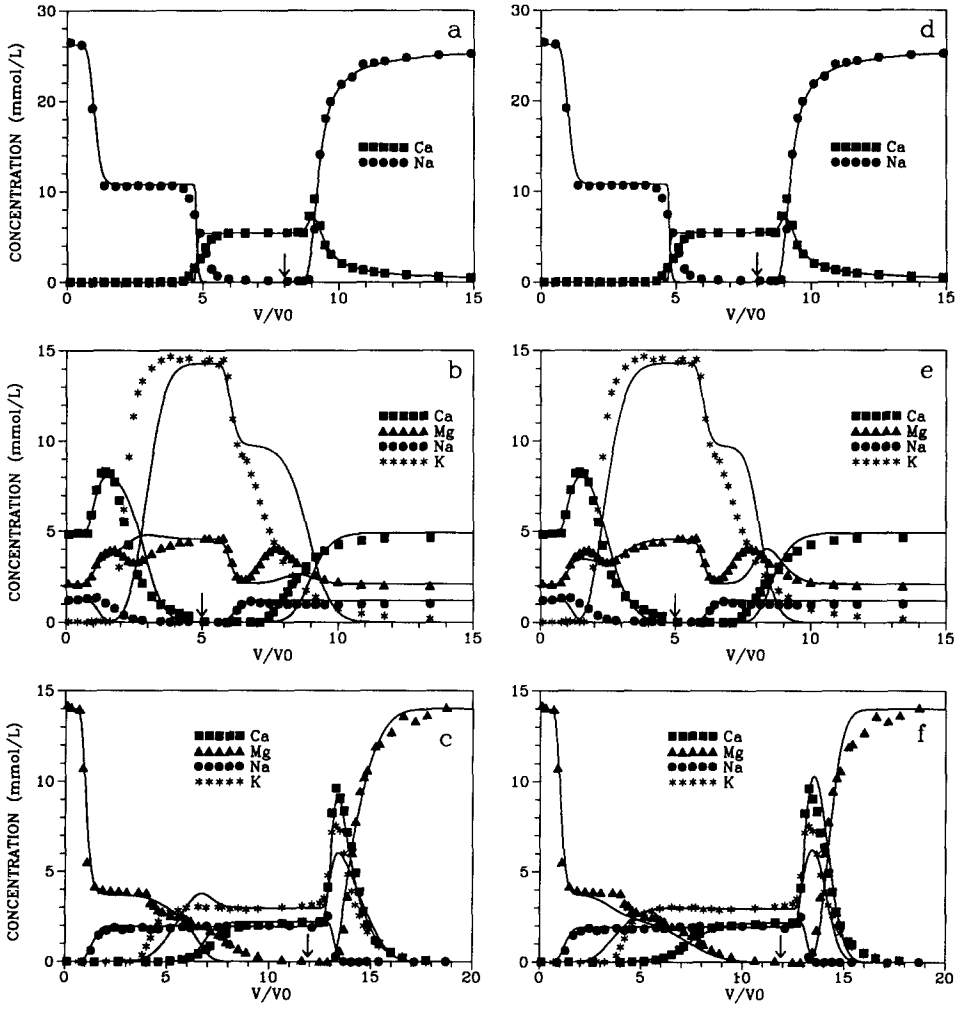

Fig. 3. Experimetal data (*symbols*) and model calculations (*solid lines*) for exchange breakthrough curves at different normality with different sets of selectivity coefficients and Pe = 50: (a) exp. *4*, set *1*; (b) exp. *8*, set *1*; (c) exp. *9*, set *1*; (d) exp. *4*, set *2*; (e) exp. *8*, set *2*; and (f) exp. *9*, set *2*.

in Fig. 1a–c (for Pe = 400). We conclude that the selectivity coefficients set *1* and arbitrarily adjusted Pe = 50 are able to describe the entire set of exps. *1–7* reasonably well.

4.2. Multicomponent exchange experiments

In order to test how well such a calibrated model is able to predict the outcome of more complicated situations, we have performed two additional multicomponent exchange experiments (see Table 1, exps. *8* and *9*). The model prediction with Pe = 50 and set *1* is shown in Fig. 3b and c, respectively. While the model captures the major trends of the breakthrough, several parts of the experimental curves show, even qualitatively, different behaviour. Particularly, the experimental records of Mg^{2+}, K^+ in Fig. 3b and K^+ in Fig. 3c are predicted in an inadequate fashion. The reason for this discrepancy can be understood as follows. In the case of such a multicomponent experiment, the shape of the breakthrough curves which involves several retarded fronts is very sensitive to the values of the selectivity coefficients. In contrast, in the case of a binary experiment, the shape of the self-broadening front changes very gradually as a function of the selectivity coefficient. Therefore, the determination of the selectivity coefficients from binary exchange experiments will be much less accurate. If selectivity coefficients determined in this fashion are used for the prediction of multicomponent experiments, one may observe substantial disagreement between the model predictions and the experiments. For this reason, we have attempted to determine all three selectivity coefficients from the single experimental record of exp. *8*. As the calculation of a single multicomponent experiment is already quite lengthy, the selectivity coefficients have been determined by trial and error. The new set of selectivity coefficients (set *2*, second row in Table 3) includes $K_{K/Na} = 10$ and $K_{Mg/Na} = 5.7$ mol L^{-1} with the value of $K_{Ca/Na} = 6.4$ mol L^{-1} unchanged. This new set can reproduce the measured breakthrough curves of exps. *8* and *9* (Fig. 3e and f) much better, even though some disagreement still remains. However, these new values of selectivity coefficients (set *2*) can reproduce exps. *1–7* almost equally well as the original set *1*. The results for Pe = 50 are shown in Fig. 3d (exp. *4*) and in Fig. 4a–f (exps. *1–3* and *5–7*). We conclude that the entire set of nine experiments can be described with one value of CEC, a single set of selectivity coefficients (set *2*) and an adjusted value of the Péclet number. Table 3 shows that the present selectivity coefficients are well comparable with values determined by other authors.

Let us now discuss the multicomponent experiments in some more detail. Consider first exp. *8* (Fig. 3e) which may be thought to mimic a landfill leachate penetrating into the soil. The soil is equilibrated with a soil solution containing Ca^{2+}, Mg^{2+} and Na^+. This solution is displaced by a solution of a higher normality containing K^+ and Mg^{2+}. In this experiment, we can observe all four fronts which are expected for this system. The first (non-retarded) front corresponds to the normality front where the normality of the solution adjusts to the final value. Just afterwards, the second front is visible in the calculated curve only as a slightly retarded decrease of the Na^+

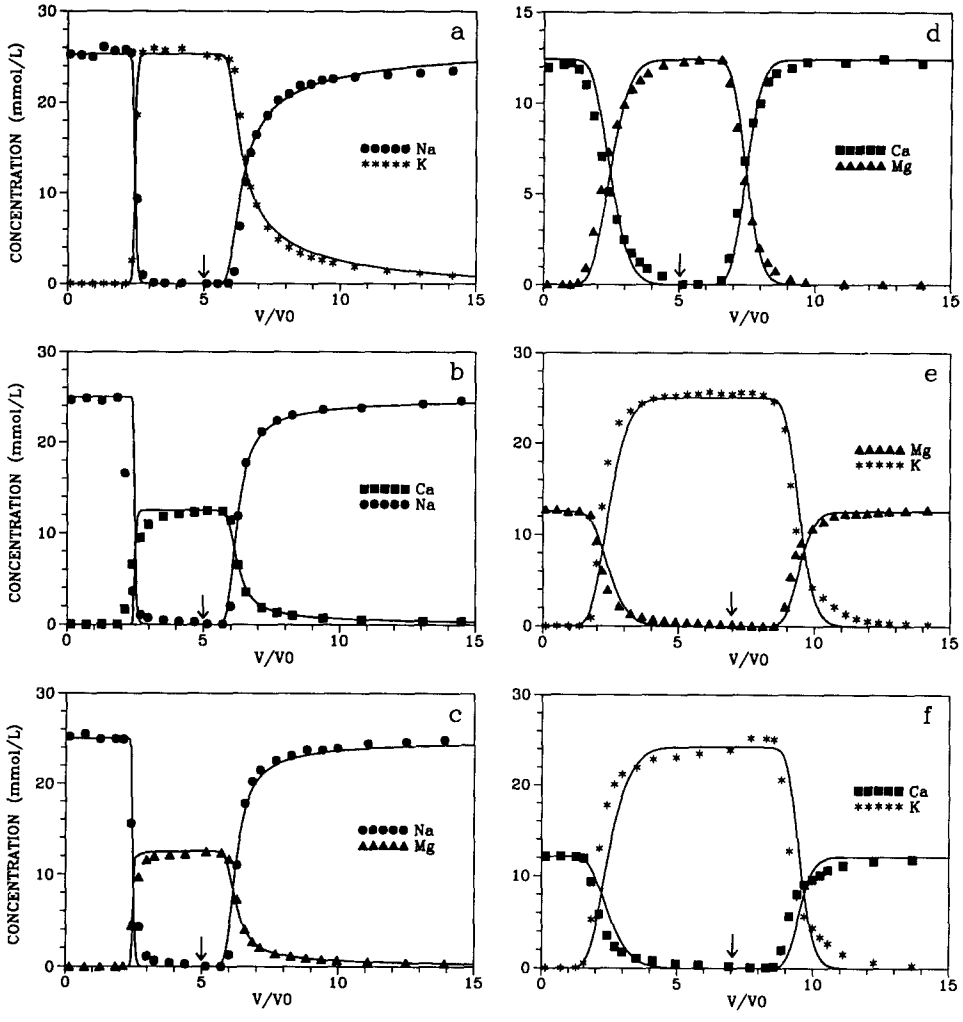

Fig. 4. Experimetal data (*symbols*) and model calculations (*solid lines*) for binary exchange breakthough curves with set *2* and Pe = 50: (a) exp. *1*; (b) exp. *2*; (c) exp. *3*; (d) exp. *5*; (e) exp. *6*; and (f) exp. *7*.

concentration. In the third front at about two pore volumes, the main part of sorbed Ca^{2+} is replaced by K^+. The fourth front (around 3.5 pore volumes) involves exchange of Ca^{2+} and Mg^{2+}. The same types of fronts can also be recognized in the reverse experiment.

In exp. *9* (Fig. 3f) the column has been saturated with Mg^{2+} and eluted with a solution containing Na^+, K^+ and Ca^{2+}. Again, four fronts are expected. After the first front, which corresponds to the normality change, the second front, which is (slightly) retarded, indicates the completion of the exchange of Mg^{2+} by Na^+. The third and fourth retarded fronts involve release of K^+ and Ca^{2+}, respectively. Note

that the cations are eluted from the column in the order of their affinity to the exchanger, Na^+ first, then K^+ and finally Ca^{2+}. In the reverse experiment, all cations are eluted soon after the normality front because the concentration of Mg^{2+} in the feed is quite high. The order of the eluted cations is the same as in the first part of the experiment.

5. Conclusions

In this article we have presented the results of a multicomponent transport study of four major cations (Na^+, K^+, Ca^{2+} and Mg^{2+}) in laboratory columns packed with a non-calcareous soil. A box model coupled to exchange equilibria is able to predict quantitatively the outcome of nine different breakthrough experiments with a reasonable accuracy. For all experiments, we have used a single set of selectivity coefficients (set *2*, Table 3), an independently verified value of cation-exchange capacity (CEC) and an adjusted value of the column Péclet number. The experimental conditions have been chosen such that complicated situations involving the simultaneous exchange of several cations are also included. We have found that the prediction of such multicomponent experiments with independently determined selectivity coefficients from binary exchange experiments (set *1*, Table 3) is quite poor. Our approach is to determine all selectivity coefficients from multicomponent experiments. The experiments could be described well with an adjusted value of the Péclet number. The Péclet number which is obtained from an independent tracer experiment is much larger and leads to predictions of the widths of sharp fronts which are much smaller than experimentally observed. We suspect that kinetic effects which can be described as an effective dispersive process are the reason of this behaviour (Bales and Szecsody, 1985; Wagner et al., 1994). Our set of parameters (selectivity coefficients set *2*, CEC and Pe) is a good one for the description of the present experimental data set within the discussed model. The residual discrepancies between experiments and model predictions could probably be explained on the basis of a more detailed description of sorption equilibria (more that one type of sites) and kinetic effects. However, we cannot entirely exclude the unlikely possibility that kinetic effects are the source of the difficulties in determining the selectivity coefficients from the binary experiments accurately.

Concepts from non-linear chromatography can be used in order to interpret all experiments in a qualitative fashion. We have been able to identify the proper number of fronts and to explain the existence of a non-retarded normality front. Neglecting dispersion effects, breakthrough curves involving a single retarded front can be understood quantitatively in a straightforward fashion without extensive numerical computations (Schweich and Sardin, 1981). In the multicomponent case (i.e. more than one retarded front) the picture becomes more complicated but still some understanding can be achieved (Helfferich and Klein, 1970; Appelo et al., 1993). In practical situations, however, some of the expected fronts can be obscured by dispersion effects.

Acknowledgements

We would like to thank to M. Sardin and D. Schweich for several enlightening discussions and for the installation of the IMPACT code. Thanks also to A. Stahel for his X-ray expertise, and to B. Buchter, C. Bürgisser, C. Hinz and J. Westall for careful reading of the manuscript.

References

Appelo, C.A.J., Willemsen, A., Beekman, H.E. and Griffioen, J., 1990. Geochemical calculations and observations on salt water intrusions, II. Validation of a geochemical model with laboratory experiments. J. Hydrol., 120: 225–250.

Appelo, C.A.J., Hendriks, J.A. and van Veldhuizen, M., 1993. Flushing factors and a sharp front solution for solute transport with multicomponent exchange. J. Hydrol., 146: 89–113.

Bajracharya, K. and Barry, D.A., 1993. Mixing cell models for nonlinear equilibrium single species adsorption and transport. J. Contam. Hydrol., 12: 227–243.

Bales, R.C. and Szecsody, J.E., 1985. Microscale processes in porous media. In: D.C. Melchior and R.L. Basset (Editors), Chemical Modeling of Aqueous Systems, II. Am. Chem. Soc., Symp. Ser. 416.

Bjerg, P.J., Ammentorp, H.C. and Christensen, T.H., 1993. Model simulations of field experiment on cation exchange-affected multicomponent solute transport in a sandy aquifer. J. Contam. Hydrol., 12: 291–311.

Bolt, G.H., 1967. Cation-exchange equations used in soil science — A review. Neth. J. Agric. Sci., 15: 81–103.

Bond, W.J. and Phillips, I.R., 1990. Cation exchange isotherms obtained with batch and misible-displacement techniques. Soil Sci. Soc. Am. J., 54: 722–728.

Bürgisser, C.S., Černík, M., Borkovec, M. and Sticher, H., 1993. Determination of nonlinear adsorption isotherms from column experiments: an alternative to batch studies. Environ. Sci. Technol., 27: 943–948.

Charbenau, R.J., 1981. Groundwater contaminant transport with adsorption and ion exchange chemistry: Method of characteristics for the case without dispersion. Water Resour. Res., 17: 705–713.

Dagan, G., 1989. Flow and Transport in Porous Formations. Springer, New York, NY.

Dufey, J.E. and Delvaux, B., 1989. Modeling potassium–calcium exchange isotherms in soils. Soil Sci. Soc. Am. J., 53: 1297–1299.

Gaston, L.A. and Selim, H.M., 1990. Predicting cation mobility in montmorillonitic media based on exchange selectivities of montmorillonite. Soil Sci. Soc. Am. J., 54: 1525–1530.

Griffioen, J., Appelo, C.A.J. and van Veldhuizen, M., 1992. Practice of chromatography: Deriving isotherms from elution curves. Soil. Sci. Soc. Am. J., 56: 1429–1437.

Helfferich, F. and Klein, G., 1970. Multicomponent Chromatography. Dekker, New York, NY.

Jardine, P.M., Wilson, G.V. and Luxmoore, R.J., 1988. Modeling the transport of inorganic ions through undisturbed soil columns from two contrasting watersheds. Soil Sci. Soc. Am. J., 52: 1252–1259.

Jauzein, M., André, C., Margrita, R., Sardin, M. and Schweich, D., 1989. A flexible computer code for modelling transport in porous media: IMPACT. Geoderma, 44: 93–113.

Mansell, R.S., Bond, W.J. and Bloom, S.A., 1993. Simulating cation transport during water flow in soil: two approaches. Soil Sci. Soc. Am. J., 57: 3–9.

Page, A.L., Miller, R.H. and Keeney D.R. (Editors), 1982. Methods of Soil Analysis, II. Chemical and Microbiological Properties. Soil Sci. Soc. Am., Madison, WI.

Rainwater, K.A., Wise, W.R. and Charbeneau, R.J., 1987. Parameter estimation through groundwater tracer tests. Water Resour. Res., 23: 1901–1910.

Sardin, M., Krebs, R. and Schweich, D., 1986. Transient mass- transport in the presence of non-linear physico-chemical interaction laws: Progressive modelling and appropriate experimental procedures. Geoderma, 38: 115–130.

Sardin, M., Schweich, D., Leij, F.J. and van Genuchten, M.Th., 1991. Modeling the nonequilibrium transport of linearly interacting solutes in porous media: A review. Water Resour. Res. 27: 2287–2307.

Schulin, R., Papritz, A., Flühler, H. and Selim, H.M., 1991. Parameter estimation for simulating binary homovalent cation transport in aggregated soils at variable ionic strength. J. Contam. Hydrol., 7: 1–19.

Schulz, H.D. and Reardon, E.J., 1983. A combined mixing cell/analytical model to describe two-dimensional reactive solute transport for unidirectional groundwater flow. Water Resour. Res., 19: 493–502.

Schweich, D. and Sardin, M., 1981. Adsorption, partition, ion exchange and chemical reaction in batch reactors or in columns — A review. J. Hydrol., 50: 1–33.

Schweich, D., Sardin, M. and Gaudet, J.-P., 1983. Measurement of a cation exchange isotherm from elution curves obtained in a soil column: Preliminary results. Soil Sci. Soc. Am. J., 47: 32–37.

Schweich, D., Sardin, M. and Jauzein, M., 1993. Properties of concentration waves in presence of nonlinear sorption, precipitation/dissolution, and homogeneous reactions, 1. Fundamentals. Water Resour. Res., 29: 723–733.

Valocchi, A.J., 1993. Impact of small-scale spatial variability upon transport of sorbing pollutants. In: D. Petruzzelli and F.G. Helfferich (Editors), Migration and Fate of Pollutants in Soils and Subsoils. Springer, Berlin.

Valocchi, A.J., Street, L.R. and Roberts, P.V., 1981. Transport of ion-exchanging solutes in groundwater: Chromatographic theory and field simulation. Water Resour. Res., 17: 1517–1527.

Villermaux, J., 1981. Theory of linear chromatography. In: A.E. Rodriques and D. Tondeur (Editors), Percolation Processes: Theory and Applications. NATO (N. Atlantic Treaty Org.), ASI (Adv. Stud. Inst.), Ser. E, Sijthoff & Noordhoff, Alphen-aan-den-Rijn.

Wagner, J., Chen, H., Brownawell, B.J. and Westall, J., 1994. The use of cationic surfactants to modify soil surfaces to promote sorption and retard migration of hydrophobic organic compounds. Environ. Sci. Technol., 28: 231–237.

Whittig, L.D. and Allardice, W.R., 1986. X-ray diffraction techniques. In: A. Klute (Editor), Methods of Soil Analysis, I. Physical and Mineralogical Methods. Soil Sci. Soc. Am., Madison, WI.

Yeh, G.T. and Tripathi, V.S., 1989. A critical evaluation of recent developments in hydrogeochemical transport models of reactive multichemical components. Water. Resour. Res., 25: 93–108.